

CP Violation Results from B Decays at BABAR

Pietro Biassoni

representing the BaBar Collaboration.¹

¹Università degli Studi and INFN Milano, via Celoria 16, I-20133 Milano, Italy.
 pietro.biassoni@mi.infn.it

In the present paper we review recent experimental results from the BABAR experiment concerning the measurement of the CKM angles. A particular highlight is given to the novel independent determination of the angle α from $B^0 \rightarrow a_1(1260)^\pm \pi^\mp$ and to the recent full-luminosity updates of several angle γ measurements.

INTRODUCTION

The measurement of CP violation (CPV) in B meson decays provides crucial tests of the Standard Model and of the Cabibbo-Kobayashi-Maskawa (CKM) matrix [1]. The angle β is experimentally measured with a precision of $O(1^\circ)$ in $B^0 \rightarrow (c\bar{c})K^0$ [2] and is not covered in this paper. The determination of angles α and γ still suffers from larger experimental uncertainties. We review results from BABAR, including the measurement of α in $B^0 \rightarrow \rho\rho$ and in the novel decay mode $B^0 \rightarrow a_1(1260)^\pm \pi^\mp$, and full-luminosity updates of several angle γ measurements.

EXPERIMENTAL TECHNIQUES

The results are based on data collected with the BABAR detector [3] at the PEP-II asymmetric-energy e^+e^- collider, at a center-of-mass energy near the $\Upsilon(4S)$ resonance.

The B meson is kinematically characterized by the variables $\Delta E \equiv E_B - \frac{1}{2}\sqrt{s}$ and $m_{ES} \equiv \sqrt{s/4 - |\vec{p}_B|^2}$, where (E_B, \vec{p}_B) is the B four-momentum vector expressed in $\Upsilon(4S)$ rest frame. The total integrated luminosity corresponds to about 468×10^6 $B\bar{B}$ pairs.

Background arises primarily from random combinations of particles in $e^+e^- \rightarrow q\bar{q}$ events ($q = u, d, s, c$), and is discriminated against $B\bar{B}$ events by using event shape variables, combined into multivariate “shape” classifiers, that are indicated with \mathcal{SC} in the following.

MEASURING α

The CKM angle α is measured in $b \rightarrow u\bar{u}d$ transition, exploiting the interference between the decay of mixed and unmixed B^0 mesons. The signal B meson (B_{CP}) is reconstructed into its decay to a CP -eigenstate, accessible from both B^0 and \bar{B}^0 . From the remaining particles in the event, we reconstruct the decay vertex of the other B meson (B_{tag}) and identify its flavor, through the analysis of its decay products [4].

The distribution of the difference $\Delta t \equiv t_{CP} - t_{tag}$ of the proper decay times of B mesons into CP -eigenstates, such as $\rho^+\rho^-$, is given by

$$f_q^{\rho\rho}(\Delta t) = \frac{e^{-|\Delta t|/\tau}}{4\tau} \{1 - q_{tag} [C \cos(\Delta m_d \Delta t) - S \sin(\Delta m_d \Delta t)]\}, \quad (1)$$

where τ is the mean B lifetime, Δm_d the $B^0 - \bar{B}^0$ mixing frequency, and $q_{tag} = +1$ (-1) if the B_{tag} decays as a B^0 (\bar{B}^0). The parameters S and C describe mixing-induced and direct CPV , respectively. Considering just tree level contributions to the process, $S = \sin(2\alpha)$ and $C = 0$. However, non negligible penguin (loop) amplitudes may contribute to $b \rightarrow u\bar{u}d$ transitions. The different strong and weak phase of the penguin amplitudes may give rise to direct CPV ($C \neq 0$), and modify S into $S = \sin(2\alpha_{eff})\sqrt{1 - C^2}$, where $\alpha_{eff} = \alpha - \Delta\alpha$, with $\Delta\alpha \neq 0$. However, $\Delta\alpha$ may be extracted via an isospin SU(2) or a flavor SU(3) analysis of the decay.

α FROM $B \rightarrow \rho\rho$

Experimental Inputs

An isospin SU(2) analysis is used to extract α in $B \rightarrow \rho\rho$ decays. The $B \rightarrow \rho\rho$ decays are $P \rightarrow VV$ transitions, where P (V) denotes a pseudoscalar (vector) meson. Hence, the decay is described by three different amplitudes, one for each helicity state, with different CP transformation properties [5]. The analysis of the angular distributions of the B meson decay products allows to extract the fraction f_L of longitudinal polarization. In the helicity formalism, the differential decay rate is

$$\frac{1}{\Gamma} \frac{d^2\Gamma}{d \cos \theta_1 d \cos \theta_2} \propto 4f_L \cos^2 \theta_1 \cos^2 \theta_2 + (1 - f_L) \sin^2 \theta_1 \sin^2 \theta_2, \quad (2)$$

where $\theta_{1(2)}$ is the helicity angle between the daughter π and the B recoil direction in the first (second) ρ rest frame. Since experimental measurements have shown the decay to be dominated by the longitudinal, CP -even polarization, a full angular analysis, that allows to separate the definite- CP contributions of the transverse polarization, is not needed.

Several inputs are needed to perform the SU(2) analysis of the $B \rightarrow \rho\rho$ decay. They are: the time-dependent (TD) parameters and branching fraction (BF) of $B^0 \rightarrow \rho^+ \rho^-$ [6, 7], BF and direct CP -asymmetry (A_{CP}) of $B^+ \rightarrow \rho^+ \rho^0$ [8], and TD parameters and BF of $B^0 \rightarrow \rho^0 \rho^0$ [9]. In Table I we summarize the results of the different $B \rightarrow \rho\rho$ analyses, and the number of $B\bar{B}^0$ pairs used in each measurement. The $B^+ \rightarrow \rho^+ \rho^0$ analysis has been updated using the final

Mode	BF (10^{-6})	f_L	$C(A_{CP})$	S	$N_{B\bar{B}}$ (10^6)
$B^0 \rightarrow \rho^+ \rho^-$	$25.5 \pm 2.1^{+3.6}_{-3.9}$	$0.992 \pm 0.024^{+0.026}_{-0.013}$	$0.01 \pm 0.15 \pm 0.06$	$-0.17 \pm 0.20^{+0.05}_{-0.06}$	383
$B^\pm \rightarrow \rho^\pm \rho^0$	$23.7 \pm 1.4 \pm 1.4$	$0.950 \pm 0.015 \pm 0.006$	$-0.054 \pm 0.055 \pm 0.010$	-	465
$B^0 \rightarrow \rho^0 \rho^0$	$0.92 \pm 0.32 \pm 0.14$	$0.75^{+0.11}_{-0.14} \pm 0.04$	$0.2 \pm 0.8 \pm 0.3$	$0.3 \pm 0.7 \pm 0.2$	465

TABLE I: Results (BF, f_L , A_{CP} , C , and S) for $B \rightarrow \rho\rho$ analyses. The number of $B\bar{B}$ pairs $N_{B\bar{B}}$ used in each analysis is also reported.

BABAR dataset. Signal yields, A_{CP} and f_L are extracted using a maximum likelihood (ML) fit to m_{ES} , ΔE , SC , and the masses and helicity angles of the ρ mesons. Multidimensional probability density functions are used to properly account for variables correlations in the background.

Determination of α

Under the isospin SU(2) symmetry, the following relations hold [10]:

$$\frac{1}{\sqrt{2}} A^{+-} = A^{+0} - A^{00}, \quad \frac{1}{\sqrt{2}} \tilde{A}^{+-} = \tilde{A}^{-0} - \tilde{A}^{00}, \quad (3)$$

where A^{ij} (\tilde{A}^{ij}) is the amplitude of $B^0(\bar{B}^0) \rightarrow \rho^i \rho^j$ process. Neglecting possible electroweak penguins (EWP) amplitudes, which do not obey SU(2) isospin symmetry, $A^{\pm 0}$ receives only tree amplitude contributions. The small A_{CP} value measured in $B^+ \rightarrow \rho^+ \rho^0$ decay indicates that the contribution from EWPs is negligible, and the isospin analysis holds within an uncertainty of $1 - 2^\circ$ [11]. Other possible isospin violation effects due to finite ρ width [12] are tested by varying the $\pi\pi$ mass window. Such effects are below the current sensitivity. If A^{+0} and \tilde{A}^{-0} are aligned with a suitable choice of phases, the relations in Eq. (3) can be represented in the complex plane by two triangles, and the phase difference between A^{+-} and \tilde{A}^{+-} is $2\Delta\alpha$. Isospin relations similar to Eq. (3) hold separately for each polarization state. However, since $f_L \sim 1$, only the analysis of CP -even longitudinal decay is performed. Constraints on the CKM angle α and on the penguin contribution $\Delta\alpha$ are obtained from a confidence level (CL) scan. Assuming the isospin-triangle relations of Eq. (3), a χ^2 for the five amplitudes ($A^{+0}, A^{+-}, A^{00}, \tilde{A}^{+-}, \tilde{A}^{00}$) is calculated from the measurements summarized in Table I, and minimized with respect to the parameters that don't enter the scan. The $1 - CL$ values are then calculated from the probability of the minimized χ^2 . Results of such a scan are reported in Fig. 1 Since the measured BFs of the several reactions satisfy $\mathcal{B}(B^+ \rightarrow \rho^+ \rho^0) \approx \mathcal{B}(\rho^+ \rho^-) \gg \mathcal{B}(B^0 \rightarrow \rho^0 \rho^0)$, the

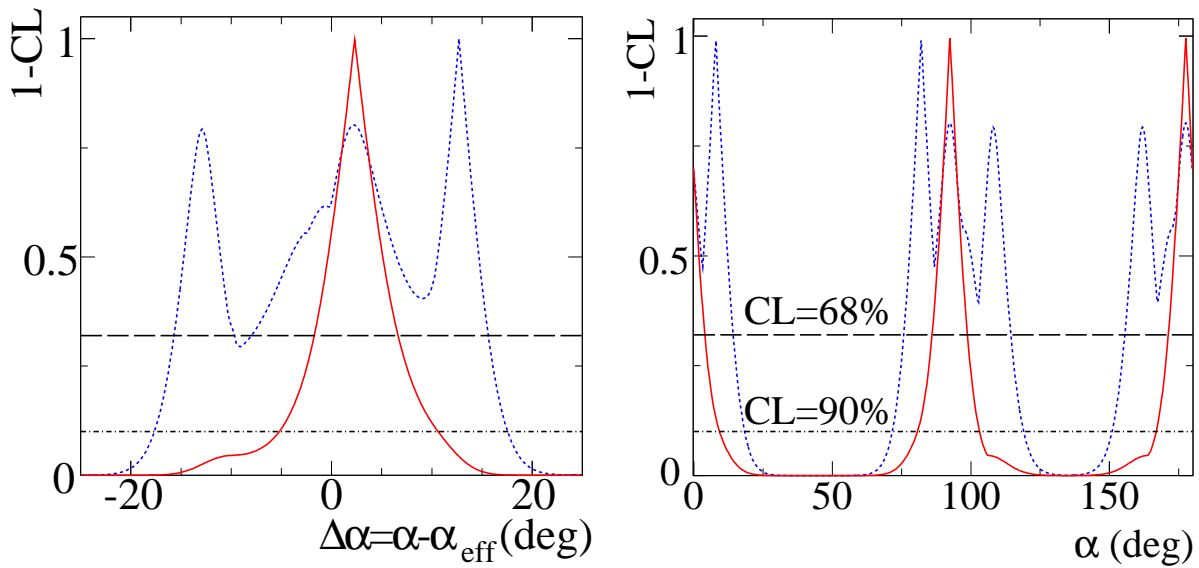


FIG. 1: Projection of the $1 - CL$ scan on (left) $\Delta\alpha$ and (right) α for the $\rho\rho$ system [8]. The red solid (blue dotted) line represents the result found using the latest [8] (previous [13]) $B \rightarrow \rho^+ \rho^0$ BF measurement.

isospin triangles do not close, *i.e.* $|A^{+-}|/\sqrt{2} + |A^{00}| < |A^{+0}|$. This results in a degeneracy of the eight-fold ambiguity on α into a four-fold ambiguity, corresponding to peaks in the vicinity of 0° , 90° (two degenerate peaks), and 180° . *BABAR* obtains a 68% CL limit $-1.8^\circ < \Delta\alpha < 6.7^\circ$. Taking only the solution consistent with the global CKM fits [14], α is equal to $92.4_{-6.5}^{+6.0}$.

α FROM $B^0 \rightarrow a_1(1260)^\pm \pi^\mp$

A novel independent measurement of α is performed by *BABAR* in the $B \rightarrow a_1(1260)^\pm \pi^\mp$ decay. The TD decay rate of the B meson into the non- CP eigenstate $a_1(1260)^\pm \pi^\mp$ is [15]

$$f_q^{a_1^\pm}(\Delta t) \propto \frac{e^{-|\Delta t|/\tau}}{4\tau} (1 \pm A_{CP}) \left\{ 1 + q_{\text{tag}} [(S \pm \Delta S) \sin(\Delta m_d \Delta t) + (C \pm \Delta C) \cos(\Delta m_d \Delta t)] \right\},$$

and α_{eff} enters this equation via $S \pm \Delta S = \sqrt{1 + (C \pm \Delta C)^2} \times \sin(2\alpha_{\text{eff}} \pm \hat{\delta})$, where $\hat{\delta}$ is the strong phase between the tree amplitudes of B^0 decays to $a_1^+ \pi^-$ and $a_1^- \pi^+$.

Experimental Inputs

Since an isospin $SU(2)$ analysis of the $B^0 \rightarrow a_1(1260)^\pm \pi^\mp$ decay is not feasible [16], a flavor- $SU(3)$ based approach is used to extract the information on $\Delta\alpha$. The experimental inputs needed for the $SU(3)$ analysis are: TD parameters and BF of $B^0 \rightarrow a_1(1260)^+ \pi^-$, BFs of $B \rightarrow a_1(1260)^\pm K$, and BF of $B \rightarrow K_{1A} \pi$. The BFs and TD parameters of $B \rightarrow a_1(1260) \pi$ and $B \rightarrow a_1(1260) K$ decays have been measured in the last few years [17, 18].

The $B \rightarrow K_{1A} \pi$ BF can be extracted using the combined branching fraction of B decays to $K_1(1400) \pi$ and $K_1(1270) \pi$, and the relative magnitude and phase of $B \rightarrow K_1(1270) \pi$ and $B \rightarrow K_1(1400) \pi$ amplitudes. $K_1(1270)$ and $K_1(1400)$ are both axial vector mesons, they have overlapping mass distributions and both decays to $K \pi \pi$, hence they undergo non-negligible interference effects. In order to include interference effects in the fit, in a recent analysis by *BABAR* [19] the K_1 system is parameterized in terms of a two-resonance, six-channel K -matrix model [20] in the P -vector approach [21]. A partial wave analysis of the diffractively produced $K \pi \pi$ system performed by the ACCMOR collaboration [20] is used to determine the decay couplings and the mass poles of the K -matrix. Signal yields are extracted using a ML fit to m_{ES} , ΔE , and \mathcal{SC} . The invariant mass of the resonant $K \pi \pi$ system is sensitive to the production parameters of the K_1 system. The combined signal branching fractions are $\mathcal{B}(B^0 \rightarrow K_1(1270)^+ \pi^- + K_1(1400)^+ \pi^-) = 31_{-7}^{+8} \times 10^{-6}$

and $\mathcal{B}(B^+ \rightarrow K_1(1270)^0 \pi^+ + K_1(1400)^0 \pi^+) = 29_{-17}^{+29} \times 10^{-6}$, where the error includes both statistical and systematic contributions. The information about the fraction and phase of the two resonances is used to calculate the contribution of the K_{1A} meson which belongs to the same SU(3) octet as the a_1 meson. The results are $\mathcal{B}(B^0 \rightarrow K_{1A}^+ \pi^-) = 14_{-10}^{+9} \times 10^{-6}$ and $\mathcal{B}(B^+ \rightarrow K_{1A}^0 \pi^+) < 36 \times 10^{-6}$, where the latter upper limit is evaluated at the 90% confidence level [19].

Determination of α

Using a flavor-SU(3) based approach, the size of penguin amplitudes contributing to the decay is related to the branching fractions of the $\Delta S = 1$ partners of the $B^0 \rightarrow a_1^\pm \pi^\mp$ decays: $B \rightarrow a_1 K$ and $B \rightarrow K_{1A} \pi$ [15, 22]. Nonfactorizable contributions to transition amplitudes from exchange and weak annihilation diagrams are neglected [15, 22]. $\hat{\delta}$ is assumed to be negligible. a_1 and K_{1A} form factors, that are needed in the analysis, are obtained from the study of τ decays [23]. A Monte Carlo method is used to derive the 68% and 90% CL upper limits for $\Delta\alpha$ [19]. The result is $|\Delta\alpha| < 11^\circ$ (13°) at the 68% (90%) CL. Combining this bound with the results from $B^0 \rightarrow a_1(1260)^\pm \pi^\mp$ TD analysis [18], the final result is $\alpha = (79 \pm 7 \pm 11)^\circ$ for the solution compatible with the CKM global fits, where the first error is statistical and systematic combined and the second is due to penguin pollution.

MEASURING γ

The CKM angle γ is measured by exploiting the interference between the $b \rightarrow c\bar{u}s$ and $b \rightarrow u\bar{c}s$ tree amplitudes in CP -violating $B \rightarrow D^{(*)} K^{(*)}$ decays. Such amplitudes also depend on the magnitude ratio $r_B \equiv \left| \frac{A(b \rightarrow u)}{A(b \rightarrow c)} \right|$, and the relative strong phase δ_B between the CKM favored and suppressed amplitudes. These hadronic parameters depend on the B decay and are extracted from data. In the following we report the results of full-luminosity updates of three different analysis [24–26], based on the GGSZ [27], ADS [28], and GLW [29] methods, respectively.

GGSZ method: $B^\pm \rightarrow D^{(*)} K^{(*)\pm}$, $D \rightarrow K_S^0 h^+ h^-$

In the GGSZ method [27], the information on γ is extracted from the Dalitz-plot distribution of the D daughters. The variables sensitive to CP violation are $x_\pm \equiv r_B \cos(\delta_B \pm \gamma)$ and $y_\pm \equiv r_B \sin(\delta_B \pm \gamma)$.

$B^\pm \rightarrow DK^\pm$, $D^* K^\pm$ ($D^* \rightarrow D\gamma$ and $D\pi^0$), and $DK^{*\pm}$ ($K^{*\pm} \rightarrow K_S^0 \pi^\pm$) decays are studied, with $D \rightarrow K_S^0 h^+ h^-$ ($h = \pi, K$) [24]. Signal yields are extracted using a ML fit to m_{ES} , ΔE , and \mathcal{SC} . A fit to the Dalitz-plot distribution of the D daughters is used to determine 2D confidence regions for x_\pm and y_\pm , which are shown in Fig. 2. The Dalitz plot model for D^0 and \bar{D}^0 decay is studied using the large ($\approx 6.2 \times 10^5$) and very pure $D^* \rightarrow D\pi$ control sample [30]. The Dalitz model includes a non-resonant part and several intermediate $K_S^0 h$ or $h^+ h^-$ quasi-two-body decays. The fitted signal yields are about 1000, 500 and 200 events for $B \rightarrow DK$, $B \rightarrow D^* K$, and $B \rightarrow DK^*$, respectively. The fitted (x_\pm, y_\pm) values are reported in Table II.

	$B^\pm \rightarrow DK^\pm$	$B^\pm \rightarrow D^* K^\pm$	$B^\pm \rightarrow DK^{*\pm}$
x_+	$-0.103 \pm 0.037 \pm 0.006 \pm 0.007$	$0.147 \pm 0.053 \pm 0.017 \pm 0.003$	$-0.151 \pm 0.083 \pm 0.029 \pm 0.006$
y_+	$-0.021 \pm 0.048 \pm 0.004 \pm 0.009$	$-0.032 \pm 0.077 \pm 0.008 \pm 0.006$	$0.045 \pm 0.106 \pm 0.036 \pm 0.008$
x_-	$0.060 \pm 0.039 \pm 0.007 \pm 0.006$	$-0.104 \pm 0.051 \pm 0.019 \pm 0.002$	$0.075 \pm 0.096 \pm 0.029 \pm 0.007$
y_-	$0.062 \pm 0.045 \pm 0.004 \pm 0.006$	$-0.052 \pm 0.063 \pm 0.009 \pm 0.007$	$0.127 \pm 0.095 \pm 0.027 \pm 0.006$
r_B	0.096 ± 0.029	$0.133_{-0.039}^{+0.042}$	$0.149_{-0.062}^{+0.066}$
$\delta_B \pmod{180^\circ}$	$(119_{-20}^{+19})^\circ$	$(-82 \pm 21)^\circ$	$(111 \pm 32)^\circ$

TABLE II: GGSZ analysis results: x_\pm , y_\pm , r_B , and δ_B . For x_\pm and y_\pm the errors are statistical, systematic and Dalitz-model, respectively. For r_B and δ_B the error is statistical and systematic combined. For $B^\pm \rightarrow DK^{*\pm}$ decay we report the value of kr_B , where $k = 0.9 \pm 0.1$ takes into account the K^* finite width.

A frequentist approach is used to obtain r_B , δ_B , and γ for each decay mode. Results of this analysis are reported in Fig. 3. The values of r_B and δ_B for each B decay mode are reported in Table II. r_B is found to be ≈ 0.1 , as expected by the theory. CKM angle γ is found to be equal to $(68 \pm 14 \pm 4 \pm 3)^\circ \pmod{180^\circ}$, where the three uncertainties are statistical, systematic and Dalitz-model, respectively. The distance d between (x_+, y_+) and (x_-, y_-) is sensitive to direct CP -violation ($d = 0$ in case of no CPV). Results of the analysis indicate a 3.5σ evidence of direct CPV .

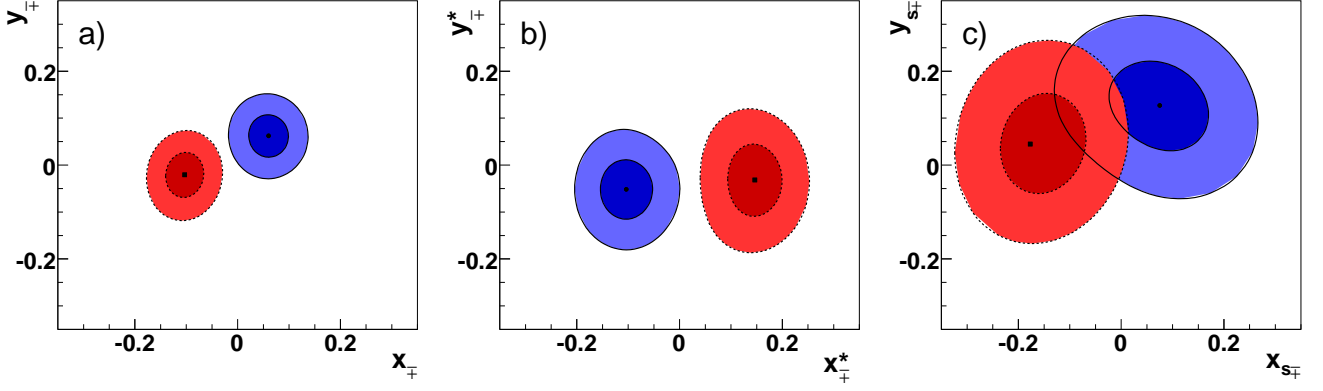


FIG. 2: 1σ and 2σ contours in the (x_{\pm}, y_{\pm}) planes for (a) $B \to DK$, (b) $B \to D^*K$ and (c) $B \to DK^*$, for B^- (solid lines) and B^+ (dotted lines) decays. (x_{\pm}^*, y_{\pm}^*) and $(x_{s\pm}, y_{s\pm})$ denote (x_{\pm}, y_{\pm}) in $B \to D^*K$ and $B \to DK^*$ decay, respectively.

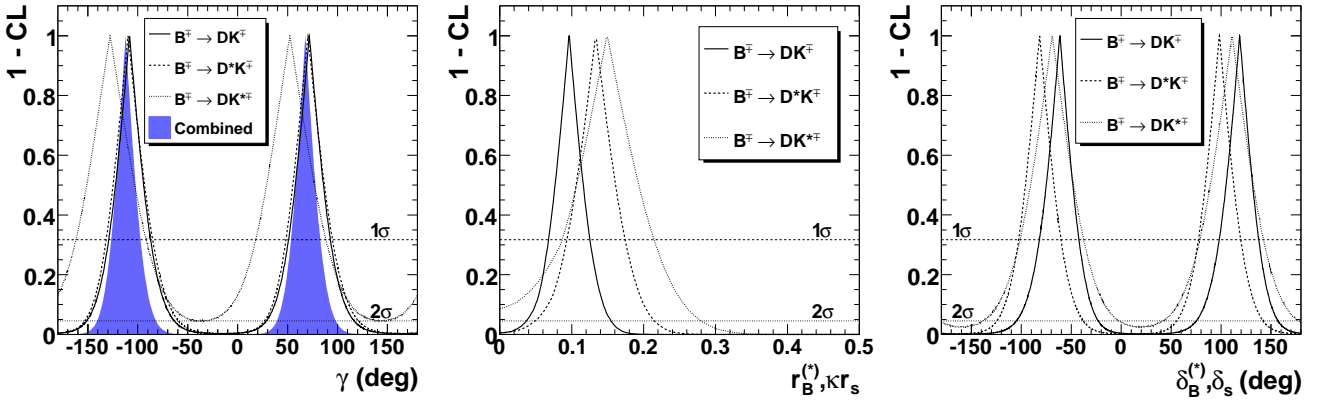


FIG. 3: 1-CL as a function of γ (left), r_B (center) and δ_B (right) from the $B \to D^{(*)}K^{(*)}$ Dalitz-plot analysis.

ADS method: $B^{\pm} \to D^{(*)}K^{\pm}$, $D \to K^{\pm}\pi^{\mp}$

The $B^{\mp} \to DK^{\mp}$ and D^*K^{\mp} ($D^* \to D\gamma$ and $D\pi^0$) decays are studied, where D^0 decays to the $K^+\pi^-$ final state [25]. Events that have same (right) sign kaons are produced in CKM favored decays. Events that have opposite (wrong) sign kaons are produced through a CKM favored (suppressed) B decay, followed by a CKM suppressed (favored) D decay. The ADS method [28] exploits the interference between these decay chains. Since the total suppression factor is equal for the two decay chains, interfering amplitudes have similar magnitude, thus large interference effects are expected. On the other side, the large suppression implies a $BF \approx O(10^{-7})$. Defining the wrong-to-right sign decay amplitude ratio $R^{\pm} \equiv \frac{\Gamma([K^{\mp}\pi^{\pm}]_D K^{\pm})}{\Gamma([K^{\pm}\pi^{\mp}]_D K^{\pm})}$, the following definitions hold

$$R_{ADS} = \frac{1}{2}(R^+ + R^-) = r_B^2 + r_D^2 \pm 2r_B r_D \cos(\delta_B + \delta_D) \cos \gamma, \quad (4)$$

$$A_{ADS} = \frac{R^- - R^+}{R^- + R^+} = \frac{2r_B r_D \sin \gamma \sin(\delta_B + \delta_D)}{R_{ADS}}, \quad (5)$$

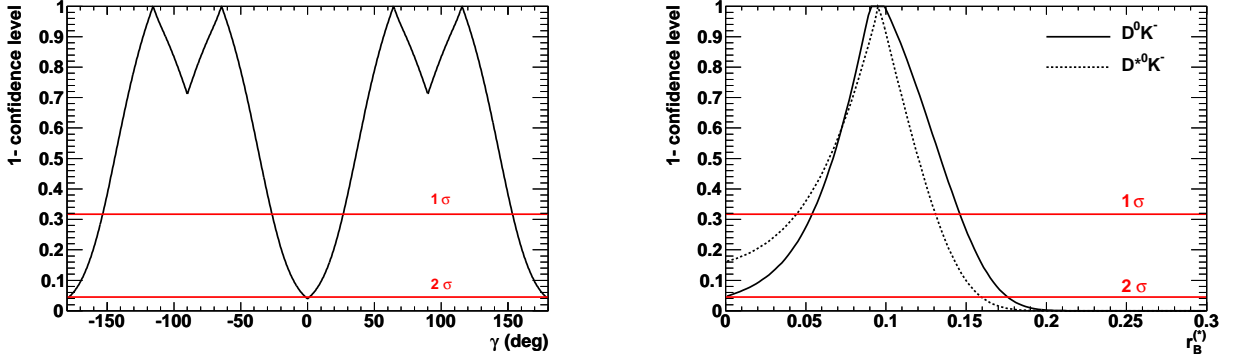
where r_D and δ_D are the ratio and the relative phase between the CKM suppressed and the CKM favored amplitude for D decay, and the $+(-)$ sign in Eq. (4) is used for D and $D^* \to D\pi^0$ ($D^* \to D\gamma$) decays.

To enhance signal purity, a tight ΔE cut is applied. Specialized selection criteria are applied to suppress $K - \pi$ misidentification and $B \to D\pi$, $D \to K^+K^-$ decays, that are the main sources of m_{ES} -peaking background. The signal yields, R_{ADS} , and A_{ADS} are determined from fits to m_{ES} and SC . In Table III we report the measured values for the signal yield, R_{ADS} , A_{ADS} , and the signal statistical significance (including systematic uncertainties), for each decay mode. A frequentist approach is used to extract the unknowns of Eq. (4)–(5) from the measured

	$B^+ \rightarrow DK^+$	$B^+ \rightarrow D_{D\pi^0}^* K^+$	$B^+ \rightarrow D_{D\gamma}^* K^+$
Wrong-sign Signal Yield	19.4 ± 9.6	10.3 ± 5.5	5.9 ± 6.4
Stat. Sign. (σ)	2.1	2.2	–
R_{ADS} (10^{-2})	$1.1 \pm 0.6 \pm 0.2$	$1.8 \pm 0.9 \pm 0.4$	$1.3 \pm 1.4 \pm 0.8$
A_{ADS}	$-0.86 \pm 0.47^{+0.12}_{-0.16}$	$+0.77 \pm 0.35 \pm 0.12$	$+0.36 \pm 0.94^{+0.25}_{-0.41}$

TABLE III: Results for $B \rightarrow DK$ ADS analysis.

observables. The values of δ_D and r_D are fixed to those reported in [31]. Results are reported in Fig. 4. Despite a poor sensitivity to γ , which is bound to be $54^\circ < \gamma < 83^\circ$, a good determination of r_B is obtained: $r_B^{DK^\pm} = 0.095^{+0.051}_{-0.041}$, $r_B^{D^*K^\pm} = 0.096^{+0.035}_{-0.051}$.

FIG. 4: 1-CL as a function of γ (left) and r_B (right) from the $B \rightarrow D^{(*)}K$ ADS study.

GLW method: $B^\pm \rightarrow DK^{(*)\pm}$, $D \rightarrow f_{(CP)}$

In the GLW method [29], the $b \rightarrow c\bar{u}s$ and $b \rightarrow u\bar{c}s$ amplitude interference is studied via D meson decays into CP eigenstates. The decay amplitudes are used to build the following quantities

$$R_{CP^\pm} = \frac{\Gamma(B^- \rightarrow D_{CP}^0 K^-) + \Gamma(B^+ \rightarrow D_{CP}^0 K^-) + \Gamma(B^- \rightarrow D^0 K^-) + \Gamma(B^+ \rightarrow \bar{D}^0 K^-)}{\Gamma(B^- \rightarrow D_{CP}^0 K^-) + \Gamma(B^+ \rightarrow D_{CP}^0 K^-)} = 1 + r_B^2 + 2\lambda_{CP} r_B \cos \gamma \cos \delta_B, \quad (6)$$

$$A_{CP^\pm} = \frac{\Gamma(B^- \rightarrow D_{CP}^0 K^-) - \Gamma(B^+ \rightarrow D_{CP}^0 K^-)}{\Gamma(B^- \rightarrow D_{CP}^0 K^-) + \Gamma(B^+ \rightarrow D_{CP}^0 K^-)} = \frac{2\lambda_{CP} r_B \sin \gamma \sin \delta_B}{R_{CP}}, \quad (7)$$

where D_{CP}^0 (D^0) indicates a D decay into a CP (flavor) eigenstate, and λ_{CP} the CP -eigenvalue of the final state. $B^\pm \rightarrow DK^\pm$ decays are reconstructed, with D mesons decaying to CP -even (K^+K^- , $\pi^+\pi^-$), CP -odd ($K_s^0\pi^0$, $K_s^0\phi$, $K_s^0\omega$), and flavor ($K^-\pi^+$) eigenstates [26]. The signal yields are measured, and the partial decay rates determined with a ML fit to m_{ES} , ΔE and \mathcal{SC} . The fitted signal yield is about 500 events for both CP -even and CP -odd final states. A_{CP^+} (A_{CP^-}) and R_{CP^+} (R_{CP^-}) are extracted from data and are equal to $0.25 \pm 0.06 \pm 0.02$ ($-0.09 \pm 0.07 \pm 0.02$) and $1.18 \pm 0.09 \pm 0.05$ ($1.07 \pm 0.08 \pm 0.04$), respectively. The four observables of Eq. (6)–(7) are used to obtain γ , r_B and δ_B , using a frequentist approach. The results are $0.24 < r_B < 0.45$ ($0.06 < r_B < 0.51$) and, modulo 180° , $11.3^\circ < \gamma < 22.7^\circ$ or $80.9^\circ < \gamma < 99.1^\circ$ or $157.3^\circ < \gamma < 168.7^\circ$ ($7.0^\circ < \gamma < 173.0^\circ$) at the 68% (95%) CL, and are shown in Fig. 5.

In order to compare these results with those from GGSZ method [24], $x_\pm = \frac{1}{4} [R_{CP^+}(1 \mp A_{CP^+}) - R_{CP^-}(1 \mp A_{CP^-})]$ is computed: $x_+ = -0.057 \pm 0.039 \pm 0.015$ and $x_- = 0.132 \pm 0.042 \pm 0.018$. Data from the $D \rightarrow K_s^0\phi$, $\phi \rightarrow K^+K^-$ decay are not used to determine x_\pm , since they are already used in the GGSZ analysis [24].

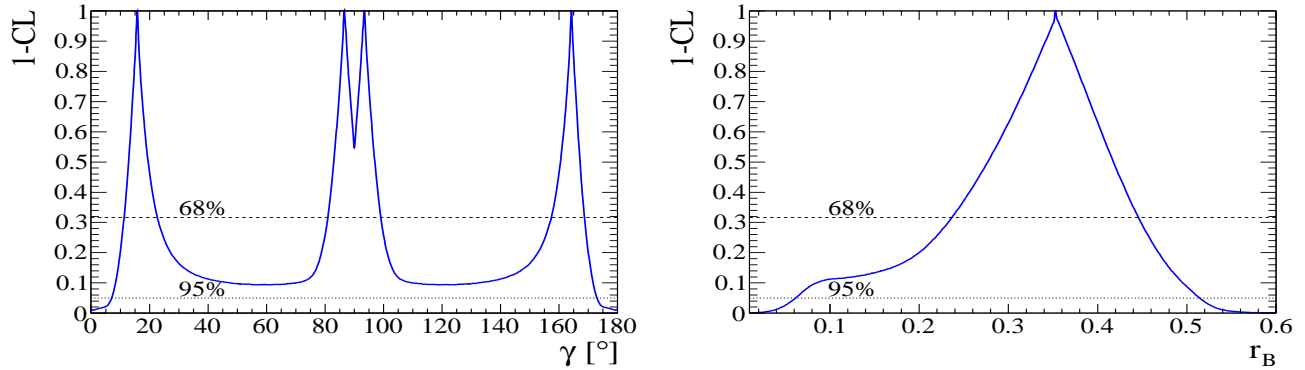


FIG. 5: 1-CL as a function of $\gamma \bmod 180^\circ$ (left) and r_B (right) from the $B \rightarrow DK$ GLW study.

CONCLUSION

We have reported results for α and γ measurement at *BABAR*. α is measured in $B \rightarrow \rho\rho$ decay at 6° level. A novel independent measurement of α in $B \rightarrow a_1(1260)\pi$ decay is performed. The measurement of angle γ using the full *BABAR* dataset is performed using three different techniques. Results of the different techniques are consistent inside the experimental uncertainties. The angle γ is measured with a precision of about 15° . The hadronic parameter r_B is found to be ≈ 0.1 , as expected by the theory. Finally, evidences of direct *CPV* at 3.5σ level are reported in $B \rightarrow D^{(*)}K$ decays.

Acknowledgments

I would like to thank all my *BABAR* collaborators and especially F. Palombo, A. Gaz, and V. Poireau for their help in preparing this paper.

-
- [1] N. Cabibbo, Phys. Rev. Lett. **10**, 531 (1963); M. Kobayashi and T. Maskawa, Prog. Theor. Phys. **49**, 652 (1973).
[2] K.-F. Chen *et al.* (Belle Collaboration), Phys. Rev. Lett. **98**, 031802 (2007); B. Aubert *et al.* (*BABAR* Collaboration), Phys. Rev. D **79**, 072009 (2009).
[3] B. Aubert *et al.* (*BABAR* Collaboration), Nucl. Instrum. Methods Phys. Res., Sect. A **479**, 1 (2002).
[4] B. Aubert *et al.* (*BABAR* Collaboration), Phys. Rev. Lett. **94**, 161803 (2005).
[5] A. L. Kagan, Phys. Lett. B **601**, 151 (2004).
[6] Charge conjugation is implied through the paper, unless otherwise specified.
[7] B. Aubert *et al.* (*BABAR* Collaboration), Phys. Rev. D **76**, 052007 (2007).
[8] B. Aubert *et al.* (*BABAR* Collaboration), Phys. Rev. Lett. **102**, 141802 (2009).
[9] B. Aubert *et al.* (*BABAR* Collaboration), Phys. Rev. D **78**, 071104R (2008).
[10] M. Gronau and D. London, Phys. Rev. Lett. **65**, 3381 (1990).
[11] M. Gronau and J. Zupan, Phys. Rev. D **71**, 074017 (2005).
[12] A. F. Falk, Z. Ligeti, Y. Nir, and H. Quinn, Phys. Rev. D **69**, 011502 (2004).
[13] B. Aubert *et al.* (*BABAR* Collaboration), Phys. Rev. Lett. **97**, 261801 (2006).
[14] J. Charles *et al.* (CKMfitter Group), Eur. Phys. J. C **41**, 1-131 (2005), updated results and plots available at <http://ckmfitter.in2p3.fr>; M. Ciuchini *et al.* (UTFIT Group), JHEP **107**, 13 (2001), updated results and plots available at <http://www.utfit.org>.
[15] M. Gronau and J. Zupan, Phys. Rev. D **73**, 057502 (2006);
[16] M. Gronau, Phys. Lett. B **265**, 389 (1991).
[17] B. Aubert *et al.* (*BABAR* Collaboration), Phys. Rev. Lett. **97**, 051802 (2006); Phys. Rev. Lett. **100**, 051803 (2008).
[18] B. Aubert *et al.* (*BABAR* Collaboration), Phys. Rev. Lett. **98**, 181803 (2007).
[19] B. Aubert *et al.* (*BABAR* Collaboration), Phys. Rev. D **81**, 052009 (2010).
[20] C. Daum *et al.* (ACCMOR Collaboration), Nucl. Phys. **B187**, 1 (1981).
[21] I. J. R. Aitchison, Nucl. Phys. A **189**, 417 (1972).
[22] M. Gronau and J. Zupan, Phys. Rev. D **70**, 074031 (2004).
[23] J. C. R. Bloch *et al.*, Phys. Rev. D **60**, 111502(R) (1999); H.-Y. Cheng and K.-C. Yang, Phys. Rev. D **76**, 114020 (2007).

- [24] P. del Amo Sanchez *et al.* (*BABAR* Collaboration), Phys. Rev. Lett. **105**, 121801 (2010).
- [25] P. del Amo Sanchez *et al.* (*BABAR* Collaboration), Phys. Rev. D **82**, 072006 (2010).
- [26] P. del Amo Sanchez *et al.* (*BABAR* Collaboration), Phys. Rev. D **82**, 072004 (2010).
- [27] A. Giri, Y. Grossman, A. Soffer and J. Zupan, Phys. Rev. D **68**, 054018 (2003).
- [28] D. Atwood, I. Dunietz and A. Soni, Phys. Rev. Lett. **78**, 3257 (1997).
- [29] M. Gronau and D. Wyler, Phys. Lett. **B265**, 172; M. Gronau and D. London, Phys. Lett. **B253**, 483 (1991).
- [30] P. del Amo Sanchez *et al.* (*BABAR* Collaboration), Phys. Rev. Lett. **105**, 081803 (2010).
- [31] E. Barbiero *et al.* (HFAG Group), “Averages of b-hadron and c-hadron Properties at the end of 2007”, arXiv:0808.1297v3.